Regionalization of Climate Elasticity Preserves Dooge's Complementary Relationship

Chandramauli Awasthi[1], Richard M. Vogel[2], and A Sankarasubramanian[1]

[1]Department of Civil, Construction, and Environmental Engineering, North Carolina State University, Raleigh, North Carolina

[2]Department of Civil and Environmental Engineering, Tufts University, Medford, Massachusetts

Corresponding author: Chandramauli Awasthi, fchandr@ncsu.edu, ORCID: 0000-0001-9826-5231

Key Points:

- Power law elasticity estimators outperform arc elasticity estimators in reproducing Dooge's complementary relationship (DCR).
- Regional elasticity estimators, hierarchical and panel models, provide both regional and at-site estimates of climate elasticity.
- Regional hierarchical model using aridity index performs the best in preserving DCR.

Abstract

Climate elasticity of streamflow represents a nondimensional measure of the sensitivity of streamflow to climatic factors. Estimation of such elasticities from observational records has become an important alternative to scenario-based methods of evaluating streamflow sensitivity to climate. Nearly all previous elasticity studies have used a definition of elasticity known as arc elasticity, which measures changes in streamflow about mean values of streamflow and climate. Using observational records in western U.S., our findings reveal that elasticity definitions based on power law models lead to both regional and basin specific estimates of elasticity which are physically more realistic than estimates based on arc elasticity. Evaluating the ability of arc and power law elasticity estimators in reproducing Dooge's complementary relationship (DCR) between potential evapotranspiration and precipitation elasticities reveal that power law elasticities estimated from at-site, panel and hierarchical statistical models reproduce DCR, whereas corresponding estimators based on arc elasticity cannot reproduce DCR. Importantly, our regional elasticity formulations using either panel and/or hierarchical formulations led to estimates of both regional and basin specific estimates of elasticities, enabling and contrasting streamflow sensitivity to climate across both basins and regions.

Plain Language Summary

Quantifying the response of streamflow of any basin with respect to climatic changes, also termed as climate elasticity of streamflow, is crucial for water resources planning and management. Developed statistical approaches, majorly based on the arc elasticity definition, have failed on multiple fronts. For example, they ignored the evapotranspiration elasticity of streamflow (ε_{PET}) estimation by being primarily focused on precipitation elasticity (ε_P), provided non-feasible positive estimates of ε_{PET}, and also failed to preserve Dooge's complementary relationship (DCR, $\varepsilon_P + \varepsilon_{PET} = 1$). In our study, we expanded on the less explored area of climate elasticity that utilizes the power law definition and developed regional (panel and hierarchical) along with widely used at-site models. We found that the models developed based on the power law definition not only provide feasible ε_{PET} estimates but also preserve DCR better than models based on the arc elasticity definition. The developed regional models showed the ability to provide both the climate elasticity estimates ($\varepsilon_P \; and \; \varepsilon_{PET}$) at regional and basin level which are reasonable and also preserve DCR.

1.0 Introduction

Understanding the sensitivity of the hydrologic cycle, particularly streamflow, to climatic factors is critical to quantify future water availability under potential climate change. One common approach to determine the sensitivity of streamflow to climatic factors is to utilize downscaled climate change projections with watershed models to estimate streamflow availability under various warming scenarios (e.g., Zhang et al. 2014, Singh et al. 2015). Unfortunately, this approach has been shown to introduce significant uncertainties due to various bias correction and downscaling techniques (Seo et al. 2016). An alternate approach is to quantify the sensitivity of observed/modeled streamflow to precipitation/temperature based on climate elasticity of streamflow, which denotes the % change in streamflow for a unit-percent change in the climatic variable of interest (Schaake, 1990; Dooge, 1992). Ever since the introduction of the concept of nondimensional climate sensitivity (or the climate elasticity) of streamflow by Schaake (1990), along with a few of its early applications by Dooge et al. (1999), Sankarasubramanian et al. (2001) and many others, there is now a considerable literature describing a myriad of approaches summarizing the non-dimensional sensitivity of watershed runoff to various hydroclimatic and watershed processes.

The two popular non-dimensional runoff elasticities are the precipitation (P) and potential evapotranspiration (PET) elasticities of runoff, which are denoted as ε_P and ε_{PET}, respectively. Compared to ε_{PET}, most studies have focused on estimating ε_P, because precipitation is the primary driver of both streamflow sensitivity (e.g., Sankarasubramanian et al. 2001, Chiew et al. 2006). Xiao et al. (2020) provide a detailed overview of the challenges in estimating ε_{PET} which stems in part due to basin-wide estimation of PET depending on variables other than temperature

(e.g., vapor pressure deficit, wind speed). Simple temperature-based PET (e.g., Hargreaves, 1975) have been shown to overestimate sensitivity of runoff under warming (Milly & Dunne, 2011) as changes in runoff depends on changes in evaporative demand as opposed to changes in temperature alone. Furthermore, since temperature is usually measured using an interval (Celsius and Fahrenheit), instead of a ratio (Kelvin) scale, resulting temperature elasticity will usually depend upon the units of temperature employed, (unless Kelvin scale is used) unlike corresponding PET and P elasticities, which are nondimensional. Thus we warn researchers not to report climate elasticities of temperature using interval scale units like Celsius or Fahrenheit because they cannot be interpreted as nondimensional elasticities and are thus would be temperature scale dependent.

Alternatively, studies have employed Budyko equations to estimate ε_{PET} (Dooge et al. 1999, Berghuijs et al. 2017). Dooge (1992) has shown that for basins with minimal human influence, a complementary relationship exists with ε_P and ε_{PET} summing to one (i.e., $\varepsilon_P + \varepsilon_{PET} = 1$). More recently, Zhou et al. (2015) show analytically that such a complementary relationship exists for any Budyko function where the evapotranspiration ratio is a function of the aridity index. Recently, Xiao et al. (2020) investigated the ability of various climate elasticity estimation methods – two water balance model-based estimators and three statistical estimators – to preserve Dooge's complementary relationship (DCR) for 84 headwater watersheds from the western US. They found, while purely statistical estimators of ε_P agreed well with model estimates, such purely statistical estimators of ε_{PET} differed substantially from model-based estimates often yielding implausible results (i.e., $\varepsilon_{PET} > 0$). Their USGS watershed-model based estimator performed better than statistical estimators, because the median of the complementary relationship was always closer to unity for the physically based models than for the statistical models. Preserving the complementary relationship certainly

adds credibility to estimates of ε_P and ε_{PET} because it ensures preservation of both the mean annual water balance (Dooge 1992) as well as the well documented and widely tested Budyko relationships (Zhou et al. 2015). It is important to use climate elasticity estimators that preserve the complementary relationship, because this will ensure that the estimates of ε_{PET} are robust even if accurate estimates of PET are difficult to obtain due to the limited data availability (e.g., humidity). Ensuring reproduction of the complementary relationship is critical because it provides a simplistic and observational data-based approach to obtain estimates of climate elasticity in contrast with traditional approaches associated with climate change studies, which only employ scenario analyses of hydrologic and climatic change. Finally, reproduction of the complementary relationship ensures reproduction of the widely tested Budyko type relationships because it also ensures reproduction of the long-term water balance as shown by Zhou et al. (2015).

Given this rationale and motivated by the initial effort of Xiao et al. (2020)'s to analyze DCR within the context of estimation of climate elasticity of streamflow, we pursue a comprehensive evaluation of elasticity estimators based on different definitions of elasticity (discussed more in the next section), but also by proposing two new regional climate elasticity estimation approaches. It has long been known that regional estimation techniques provide more credible estimates of various hydroclimatic characteristics (Vogel et al., 1998, 1999), and more credible estimates of watershed model parameters (Fernandez et al., 2000) than at-site estimation methods. This is because regional methods add hydroclimatic information by augmenting limited 'at-site' data sets with regional information and other basin characteristics to explain across-basin differences within a region (Fang et al., 2023). Regionalization also provides a basis for developing more comprehensive spatio-temporal models for forecasting

streamflow and their sensitivities (Johsnon et al., 2023; Fang et al., 2023). Hence, another critical element of our study relates to our recommendation to go beyond at-site estimation of climate elasticity and instead we evaluate the use regional estimators of precipitation (P) and potential evapotranspiration (PET) elasticities and evaluate their ability to preserve the DCR by comparing them with at-site estimators. Thus our overall study objectives are to a) evaluate the ability of various at-site and regional statistical estimators of P and PET elasticity of streamflow for their ability to reproduce the DCR, b) evaluate the behavior of those estimates of P and PET elasticities which are shown to reproduce the DCR, in terms of how they vary across selected headwater watersheds (Xiao et al., 2020) in western Pacific States, c) determination of which physical basin characteristics control whether or not a particular estimator is able to preserve the DCR, and d) evaluate estimators of P and PET elasticities based on two different definitions of climate elasticity, arc elasticity and power law elasticity, for their ability to reproduce DCR and produce estimates of climate elasticity which are in accord with results from physical models. In Section 2, we describe the elasticity concept and DCR as well as various elasticity definitions and estimators commonly used along with the data set employed in our experiments. Section 3 proposes several new at-site and regional estimators of climate elasticities. Results and discussion are provided in section 4, with conclusions in section 5.

2.0 Background and Data

2.1 Background – Elasticity Definition and Model Forms

The concept of nondimensional sensitivity or elasticity is widely used for describing the sensitivity of economic demand and supply to various factors (Kirschen et al., 2000; Andreyeva et

158 al., 2010). Schaake (1990) evaluated the sensitivity of streamflow to changes in climate and
159 introduced the concept of climate elasticity in hydrology. The climate elasticity of streamflow is a
160 measure of relative change in streamflow Q for a relative change in any given climatic variable.
161 Thus, for any climatic variable, for instance precipitation P, precipitation elasticity of streamflow
162 can be defined as

163 $$\varepsilon_P = \frac{\partial Q/Q}{\partial P/P} = \frac{\partial Q}{\partial P}\,\frac{P}{Q} \qquad (1)$$

164 The elasticities of other climatic variables can also be defined in a similar fashion. There are
165 numerous approaches to the definition and estimation of elasticities as described in section 3 of
166 Sankarasubramanian et al. (2001). A common approach is to estimate the terms in (1) using their
167 mean values of the climatic and streamflow variables $(\bar{P}, \bar{Q})$. Elasticity defined at the means of
168 variables, yields what Lerner (1933) terms the arc elasticity, definition of elasticity which can be
169 expressed as

170 $$\varepsilon_P = \left(\frac{dQ}{dP}\right)_{\bar{P},\bar{Q}}\,\frac{\bar{P}}{\bar{Q}} = \frac{(Q-\bar{Q})}{(P-\bar{P})}\,\frac{\bar{P}}{\bar{Q}} \qquad (2)$$

171 Allaire et al. (2015) show how to combine the arc elasticity (2) with the chain rule to derive
172 generalized multivariate models of arc elasticity. Lerner (1933) discussed difficulties associated
173 with the arc elasticity definition over a discrete range of the variables of interest, and as is shown
174 later, we confirm his concerns.

175 A value of two for precipitation elasticity in either (1) or (2) implies that a 1% increase in long
176 term watershed precipitation will lead to a 2% increase in long term watershed runoff. The arc
177 elasticity definition in (2) has been used by most of the studies on climate elasticity in hydrology
178 (Sankarsubramanian et al., 2001; Allaire et al. 2015; Andreassian et al., 2016; Xiao et al., 2020).

Some of these studies also considered PET as an additional climate variable and developed a tri-variate linear regression model in (3), where $\overline{PET}$ is mean of PET and ϵ is model residual.

$$\frac{Q-\bar{Q}}{\bar{Q}} = \varepsilon_P \frac{P-\bar{P}}{\bar{P}} + \varepsilon_{PET} \frac{PET-\overline{PET}}{\overline{PET}} + \epsilon \quad (3)$$

See Allaire et al. (2015) for a derivation of (3) resulting from a combination of arc elasticity definition in (2) with the chain rule. We highlight that there is no intercept in the model in (3), which is proven in Allaire et al. (2015).

The concept of elasticity is used widely in the field of economics for determining the sensitivity of demand for a product to its price, termed price elasticity. A widely used approach to elasticity estimation in economics involves the power-law definition of elasticity as described below instead of the arc elasticity. See section titled "Climate Elasticity of Streamflow" in Vogel et al. (1999) for an example of power-law approach in hydrology as well as the more recent study by Bassiouni et al, (2016). The power-law approach to elasticity relates streamflow Q with precipitation P and potential evapotranspiration PET using the power law relation $Q = \alpha P^{\beta} PET^{\gamma}$ where β and γ denote the values of ε_P and ε_{PET}, respectively, each defined by the elasticity definition in (1). A log-linear regression model form can be obtained by taking the natural log of the power law model which leads to

$$\ln(Q) = \ln(\alpha) + \varepsilon_P \ln(P) + \varepsilon_{PET} \ln(PET) + v \quad (4)$$

where v is regression model residual which ideally, should be normally distributed, independent and homoscedastic to enable statistical inference on the resulting model parameter estimates which are the elasticities of interest. We highlight that an intercept term is required for the power-law definition of elasticities in (4), whereas it is not required in the arc elasticity definitions of elasticities in (3).

Dooge's complementary relationship of climate elasticities

Dooge (1992) and Zhou et al. (2015) document two general conditions under which the elasticities in equations (3) and (4) sum to unity. The first condition is that a long-term water balance holds, so that over a particular time horizon, long-term watershed runoff is equal to the difference between mean annual precipitation and evapotranspiration assuming negligible changes in watershed storage (Sankarasubramanian et al. 2020). The second condition is that the Budyko hypothesis holds, which can be represented by the functional relationship.

$$\frac{\overline{AET}}{\overline{PET}} = \Phi\left(\frac{\bar{P}}{\overline{PET}}\right) \qquad (5)$$

where $\overline{AET}$ is the long-term mean of actual evapotranspiration, the ratio of $\frac{\bar{P}}{\overline{PET}}$ is termed as the wetness or humidity index, and Φ is a homogeneous function which depends only on the humidity index. Instead of the humidity index, the Budyko relationship can also be defined in terms of the aridity index (AI) which is simply the inverse of the humidity index so that $AI = \frac{\overline{PET}}{\bar{P}}$. The Budyko hypothesis in equation (5) has received considerable attention due in part to the increased focus on the effects of climate change on water resource systems and has been verified in thousands of natural watersheds across the globe (for recent reviews see Padron et al. 2017; and Sankarasubramanian et al. 2020). Interestingly, Zhou et al. (2015) document how climate elasticities can be used to generate a wide range of plausible Budyko type functions in (5).

Under both above assumptions, Dooge's (1992) complementary relationship (DCR) can be written as

$$\varepsilon_P + \varepsilon_{PET} = 1 \qquad (6)$$

Preserving DCR is critical as it ensures preservation of the long-term water balance. Given the extensive literature on estimation of ε_P and ε_{PET}, it is surprising that other than the recent study by Xiao et al. (2020), we are not aware any other studies that have analyzed the challenges in reproduction of the complementary relationship in (6), especially within the context of evaluating the climate sensitivity of streamflow.

2.2 Estimators of Climate Elasticity

Three different approaches exist for estimating climate elasticity of streamflow: (1) a watershed model-based approach, (2) analytical methods based on the Budyko relationship, and (3) statistical approaches. For a brief review of the variety of approaches for estimation of climate elasticities see Table 1 in Wang et al. (2016).

The watershed model-based approach involves calibration of a rainfall-runoff model followed by perturbation of the climatic inputs to estimate corresponding changes in streamflow regimes. While this approach is generally preferred due to its physical basis, results can differ remarkably, even when the same model is applied to the same watershed by different investigators, due to uncertainty in model inputs, model structure and parameter estimation (for example, see Table 1 in Sankarasubramanian et al., 2001). Analytical approaches based on the Budyko relationship involve derivation of the necessary partial derivatives of (5) to obtain analytic expressions for the climate elasticities (e.g., Dooge (1992), Xu et al. (2014) and Wang et al. (2016)).

In contrast, empirical statistical approaches are much easier to implement than watershed model-based approaches, however they lack a physical basis (e.g., Andreassian et al., 2016; Konapala and Mishra, 2016; and Xiao et al., 2020). A review of the literature reveals that with the exception of Vogel et al. (1999) and Bassiouni et al. (2016) most previous statistical approaches

to estimating climate elasticities of streamflow employ arc elasticities estimated using some form of regression such as either ordinary least square (OLS) or generalized least square (GLS) regression (e.g., Andreassian et al. (2016) and Xiao et al. (2020)). Sankarasubramanian et al. (2001) briefly discussed power law elasticity estimates yet most of their results employed the arc elasticity approach. In a recent comparison of the precipitation and potential evapotranspiration elasticities of runoff in the western U.S. using arc elasticity, Xiao et al. (2020) found that even the most sophisticated multivariate GLS statistical methods recommended by Andreassian et al. (2016) and Konapala and Mishra (2016) for estimating such arc climate elasticities were unable to reproduce the DCR in (6).

2.3 Hydroclimatic Data

Following Xiao et al. (2020) we consider 84 headwater river basins in the western U.S. after implementing various screening criteria for the GAGES-II (Geospatial Attributes of Gages for Evaluating Streamflow) data set (https://water.usgs.gov/GIS/metadata/usgswrd/XML/gagesII_Sept2011.xml). Our screening criteria are based on the degree of upstream regulation, missing streamflow record, and anthropogenic disturbances of the basin. This results in the selection of 24 basins in California, 23 basins in Oregon, and 37 basins in Washington after the screening. The screening criterion is given in detail in Xiao et al. (2020), and the selected watersheds are also the same for this study which enables us to compare the performance of power law elasticities advocated here with the arc elasticities employed by Xiao et al. (2020).

The average daily streamflow data of the selected gages was retrieved from the U.S. Geological Survey (USGS) water data set (https://waterdata.usgs.gov/nwis/). The daily flows are summed to obtain total annual runoff for different water years. To obtain the drainage area (DA) and elevation

(EL) of these basins, we employed the R-package "dataRetrieval" from the USGS (Hirsch and Cicco, 2015). For our model calibration, we obtained total annual precipitation from the University of Washington's Surface Water Monitor (SWM; Wood and Lettenmaier, 2006) gridded data set. Estimates of PET are based on Penman-Monteith (Penman, 1948) using temperature, net radiation, vapor pressure deficit, and wind speed as inputs (see Xiao et al., 2020). Using annual P and PET values, we estimated the mean annual aridity index (AI). We also estimated Pearson's correlation coefficient (CR) between P and PET suggesting the phase relationship between moisture and energy availability in different basins. We show the spatial variation of four basin attributes (AI, CR, EL, DA) on the U.S. map (Figure 1). It can be noted that humid basins located in the northwest region have relatively lower elevations, smaller drainage areas, and very poor correlation between energy and moisture than the more arid southern regions. Most of the basins located away from the coast have higher elevations with an average basin elevation of more than 4000 ft.

3.0 Methods – At-site and Regional Estimators of Climate Elasticity

We consider three different classes of climate elasticities of runoff ($\varepsilon_P, \varepsilon_{PET}$), one at-site and two regional estimators based on the two different definitions of elasticity: arc elasticity given in equation 3 and power law elasticity given in equation 4. Three different approaches are employed to estimate both arc and power law elasticities, (1) at-site OLS estimators, as well as two regional elasticity estimators based on (2) panel regression and (3) hierarchical regression. The regional estimators of elasticity pool the dataset from all 84 basins together and elasticities for all the basins are obtained in one single regional estimation procedure. Let Q_{ij} be the annual streamflow in a water year j for a given basin i, P_{ij} and PET_{ij} are the corresponding annual precipitation and potential evapotranspiration. ε_{P_i} and ε_{PET_i} are the precipitation elasticity and potential evapotranspiration elasticity for basin i, and ϵ_{ij} is resulting model residual for the selected model.

All models giving arc elasticities are denoted with prefix 'Arc' while models giving power law elasticity estimates are denoted with prefix 'Log' in the manuscript.

3.1 At-site OLS Model

The at-site OLS arc elasticity and power law elasticity estimators correspond to the Arc and power law elasticity definitions in equations (3) and (4) and are summarized below in equations 7a and 7b, respectively. The model coefficients are the climate elasticity estimates, which can be obtained by regressing model predictand with the predictors for each basin ($i = 1, 2, \dots, 84$). Resulting elasticity models, termed as Arc-OLS (7a) and Log-OLS (7b), are calibrated using the 'lm' function in R programming language.

$$\left(\frac{Q_{ij} - \overline{Q_{iJ}}}{\overline{Q_{iJ}}}\right) = \varepsilon_{Pi}\left(\frac{P_{ij} - \overline{P_{iJ}}}{\overline{P_{iJ}}}\right) + \varepsilon_{PETi}\left(\frac{PET_{ij} - \overline{PET_{iJ}}}{\overline{PET_{iJ}}}\right) + \epsilon_{ij} \quad (7a)$$

$$\ln(Q_{ij}) = \varepsilon_{Pi}\ln(P_{ij}) + \varepsilon_{PETi}\ln(PET_{ij}) + \epsilon_{ij} \quad (7b)$$

We note that equations (7a) and (7b) are simply empirical estimators derived from the expressions for arc and power law elasticities defined in equations (3) and (4) respectively.

3.2 Regional Panel Model

Panel models are attractive because they enable the development of a single multivariate statistical model which can capture variations in both space and time, simultaneously (Yaffee, 2003). A panel or spatial model is quite different from previous multivariate climate elasticity estimation approaches which have ignored spatial variations in streamflow and climate. The spatial dimension is integral to a panel model by because a panel model is a multivariate regression model which relates time series of the dependent streamflow series at many watersheds to time series of the various watershed and climatic predictor variables. While panel models have a long and rich history in the field of econometrics for modeling multivariate relationships among time series in

311 space, their application to the field of hydrology and water resources is in its infancy (see
312 Steinschneider et al. 2013; Bassiouni et al. 2016). For example, panel approaches have been used
313 to document the influence of drought on economic growth (Brown et al. 2011), the effect of
314 urbanization on flood frequency (Over et al. 2016; and Blum et al. 2020), the impact of forest
315 cover on flood frequency (Ferreira and Ghimire, 2012), the impact of deforestation on streamflow
316 (Levy et al., 2018), the impact of rainfall on low streamflow (Bassiouni et al., 2016), prediction of
317 groundwater levels (Izady et al., 2012), residential water demand modeling (Worthington et al.
318 2009), and for determining the impact of urbanization on annual runoff coefficients
319 (Steinschneider et al., 2013). Bassouni et al. (2016) used a power law definition of elasticity to
320 obtain OLS at-site estimates of rainfall elasticity to low streamflow at watersheds in Hawaii, and
321 then they fit panel models to relate those rainfall elasticities of low streamflow across basins to
322 time series of various corresponding watershed and basin characteristics in the region. Thus there
323 is some overlap in our methodology with that of Bassouuni et al. (2016) regarding the use of power
324 law definition of elasticities and use of panel models, yet our panel models differ substantially
325 from theirs. To our knowledge, this is the first application of panel models to estimate both regional
326 and at-site estimates of climate elasticity of streamflow. Our panel model formulation described
327 below is unique and different from previous panel formulations described above, because it can
328 disaggregate the impact of regional and at-site effects on climate elasticities of streamflow.

329 We propose a panel model for the arc elasticity, termed Arc-Panel (8a), and power law
330 elasticity, termed as Log-Panel (8b).

$$\left(\frac{Q_{ij} - \overline{Q_{\iota J}}}{\overline{Q_{\iota J}}}\right) = \varepsilon_P^R \left(\frac{P_{ij} - \overline{P_{\iota J}}}{\overline{P_{\iota J}}}\right) + \varepsilon_{PET}^R \left(\frac{PET_{ij} - \overline{PET_{\iota J}}}{\overline{PET_{\iota J}}}\right) + \varepsilon_{oi} + \varepsilon_{Pi}^b \left(\frac{P_{ij} - \overline{P_{\iota J}}}{\overline{P_{\iota J}}}\right) + \varepsilon_{PETi}^b \left(\frac{PET_{ij} - \overline{PET_{\iota J}}}{\overline{PET_{\iota J}}}\right) + \in_{ij} \quad (8a)$$

$$\ln(Q_{ij}) = \varepsilon_P^R \ln(P_{ij}) + \varepsilon_{PET}^R \ln(PET_{ij}) + \varepsilon_{oi} + \varepsilon_{Pi}^b \ln(P_{ij}) + \varepsilon_{PETi}^b \ln(PET_{ij}) + \in_{ij} \quad (8b)$$

Fixed effect terms (ε_P^R and ε_{PET}^R) represent the mean estimate of the basins' regional response to precipitation and PET and is indicated by the R superscript. Basin specific deviation from the regional mean term is given by the random effects and is indicated by the b superscript in each model. In the above models, a fixed intercept is not considered to keep it similar to the at-site OLS models and because the derivation in Allaire et al. (2015) shows that when one combines an arc elasticity definition with the chain rule results in the expression shown in (8a) which has no intercept term. The model has a random basin intercept term given by ε_{oi}. The deviation of climate elasticity of individual basins from the regional mean are denoted by the ε_{Pi}^b and ε_{PETi}^b model coefficients, while $\in_{ij}$ is model residual such that $\in_{ij} \sim N(0, \sigma_e^2)$. By design, all three random effect terms also follow a multivariate normal distribution with zero mean and a model estimated variance-covariance structure. Different variance-covariance structures are possible for the random effect terms that a panel model can follow. In our study, we let the panel model follow an unstructured variance-covariance matrix that gives more flexibility to our model. Steinschneider et al. (2013) have described the panel model formulation and its coefficient estimation technique in more detail. The model parameters' estimation is based on maximum likelihood estimation (MLE) technique (Steinschneider et al., 2013). In a panel model, if the model residuals follow a homoscedastic normal distribution, and the covariance is correctly specified, then MLE estimator

is the uniformly minimum variance unbiased estimator (UMVUE) and resulting elasticity estimates will also follow a normal distribution.

We used the 'lme' function of 'nlme' R-package (Pinheiro et al., 2021) to develop and calibrate our panel models in R studio. After the model calibration, the climate elasticity value for any basin i can be obtained by adding fixed-effect term and basin specific random effect term. Hence, the final precipitation elasticity for a given basin will be $\varepsilon_{Pi} = \varepsilon_P^R + \varepsilon_{Pi}^b$, and potential evapotranspiration elasticity will be $\varepsilon_{PETi} = \varepsilon_{PET}^R + \varepsilon_{PETi}^b$.

3.3 Regional Hierarchical Model

Goldstein (2011) and Leeuw et al. (2008) describe the concept of multi-level linear models, also known as hierarchical models. Our proposed hierarchical model has two levels with the first level appearing similar to an at-site OLS model (7) and the second hierarchical level yielding regression model forms similar to the panel model (8), except that individual effects are not random but instead are explained by basin attributes. The model takes the pooled data of all 84 basins together, and resulting panel model parameter estimates provide both regional and at-site estimates of climate elasticity for the pooled data set.

We hypothesize that variations in climate elasticity of runoff across basins can be explained by basin and hydroclimatic characteristics X_i, hence we hypothesize that $\varepsilon_{Pi}^b = \alpha_P X_i$, $\varepsilon_{PETi}^b = \alpha_{PET} X_i$, and $\varepsilon_{oi}^b = \alpha_o X_i$. A full hierarchical model is proposed for arc elasticity, Arc-Hierarchical model (9a), and for power law elasticity, Log-Hierarchical model (9b).

$$\left(\frac{Q_{ij} - \overline{Q_{ij}}}{\overline{Q_{ij}}}\right) = \alpha_o X_i + \varepsilon_P^R \left(\frac{P_{ij} - \overline{P_{ij}}}{\overline{P_{ij}}}\right) + \varepsilon_{PET}^R \left(\frac{PET_{ij} - \overline{PET_{ij}}}{\overline{PET_{ij}}}\right) + \alpha_P X_i \left(\frac{P_{ij} - \overline{P_{ij}}}{\overline{P_{ij}}}\right) + \alpha_{PET} X_i \left(\frac{PET_{ij} - \overline{PET_{ij}}}{\overline{PET_{ij}}}\right) + \in_{ij} \quad (9a)$$

$$\ln(Q_{ij}) = \alpha_o X_i + \varepsilon_P^R \ln(P_{ij}) + \varepsilon_{PET}^R \ln(PET_{ij}) + \alpha_P X_i \ln(P_{ij}) + \alpha_{PET} X_i \ln(PET_{ij}) + \in_{ij} \quad (9b)$$

We evaluated the relationship between the three elasticity estimates ε_P, ε_{PET}, and DCR ($\varepsilon_P + \varepsilon_{PET}$) obtained by the USGS watershed model of Xiao et al. (2020) with the four basin attributes – mean annual aridity index (AI_i), gage elevation (EL_i), basin drainage area (DA_i), and moisture-energy phase difference, which is denoted by the Pearson's correlation coefficient between monthly P and PET (CR_i) (Figure S1). We note that all three elasticity estimates show some correlation with the aridity index, elevation, drainage area and moisture-energy phase difference, thus we considered these four basin attributes as model covariates (X_i) in the hierarchical model. We developed the hierarchical models given in (9) in R studio platform and estimated all the model coefficients with the least square estimator employed by the in-built 'lm' function. For any basin i, the final estimate of precipitation elasticity is given by $\varepsilon_P^R + \alpha_P X_i$, and elasticity for potential evapotranspiration is given by $\varepsilon_{PET}^R + \alpha_{PET} X_i$ where X_i represents hydroclimatic characteristic for the i^{th} basin.

3.4 Model Performance Evaluation

Overall, the arc and power law definitions of climate elasticities obtained for the three classes of estimators (OLS, Panel, Hierarchical) yield six different estimates of elasticities which are compared based on two metrics: 1. Goodness-of-fit or ability of model to predict respective model

predictand, and 2. models' ability to preserve the DCR. To compare the models' predictability and goodness-of-fit, we used R-squared (aka coefficient of determination).

To check the selected approach to preserve the DCR, we summed the precipitation and potential evapotranspiration elasticities and then subtracted 1 from it. This provides the information on how much a model deviates from the DCR ($\varepsilon_{Pi} + \varepsilon_{PETi} - 1$) across the 84 basins. We then estimated average absolute relative error ($AARE$) of this deviation from 1 for all 84 basins combined as given in (10). Given our main objective is to determine which statistical model best preserves the Dooge's complementary relationship, we consider $AARE$ as the key metric in selecting the best approach for estimation of the P and PET elasticities.

$$AARE = \frac{1}{84}\sum_{i=1}^{84} |(\varepsilon_{Pi} + \varepsilon_{PETi} - 1)|/1 \qquad (10)$$

Interestingly, as is shown below, the arc elasticities computed from statistical methods are all highly biased and unrealistic compared with those obtained using power law elasticities, thus we emphasize agreement of DCR for the power law elasticities, because a major finding of our work reveals that arc elasticities can be very misleading, especially when contrasted with either power law elasticities or arc elasticities obtained from a physical model such as that used in Xiao et al. (2020).

4.0 Results

Overall, we developed and calibrated a total of twelve models, six models each for the two different elasticity definitions (arc and power law), with each elasticity having one at-site OLS model, one Panel model and four hierarchical models. The performance of these models is compared in Table 1 based on the metrics $AARE$ in (10) and R^2. It should be noted that R^2 values shown are computed after considering the model residuals from all 84 basins together. Overall,

411 the message in Table 1 is that the only climate elasticity estimates which are physically plausible
412 are those which agree with the results of the physically based modeling study by Xiao et al. (2020)
413 which yields an $AARE$ = 0.084. Thus, it is only the power law elasticity results for the At-site
414 (OLS), Panel Model and the Hierarchical Model with (X: log-Aridity Index or AI) that yield
415 plausible values of $AARE$ competitive with the results of the physically based modeling approach.
416 The values of $AARE$ for all arc elasticities reported in Table 1 indicate that statistical methods of
417 estimation of arc elasticity perform poorly and in general, power law elasticities are recommended.
418 Of the recommended power law elasticities, clearly the hierarchical models only perform well in
419 terms of $AARE$ for the case when aridity index AI, is used, another important finding.

420 Figure 2 provides the distribution of climate elasticity estimates of the considered basins using
421 boxplots for at-site OLS, Panel and Hierarchical models based on the two definitions of elasticity
422 (Figure 2). Since the hierarchical model with aridity index performed better than the remaining
423 three hierarchical models, we selected only that hierarchical model for the comparison. The
424 distribution of precipitation elasticity of streamflow (Figure 2a) has similar median values for
425 OLS, Panel, Log-OLS, and Log-Panel models. Hierarchical (AI) (Log-Hierarchical (AI)) has
426 slightly lower (higher) median values. We see that overall, all six models agree for precipitation
427 elasticity estimates, though the power law elasticities exhibit significantly lower variance across
428 basins within the overall region. For PET elasticity of streamflow estimates (Figure 2b), we
429 observed that arc elasticities are generally much higher than power law elasticities. We note that
430 all three arc elasticity estimates exhibit 50% or more basins with positive estimates of ε_{PET} which
431 is physically unrealistic. In contrast, all three-power law elasticities ε_{PET} resulted in negative
432 values for most of the basins, particularly Log-Hierarchical (AI) model which estimated negative
433 $\hat{\varepsilon}_{PET}$ for all 84 basins. In Figure 2c, both the elasticities (ε_P and ε_{PET}) are added for each basin to

434 check for models' performance in capturing Dooge's complementarity, and we found again that
435 all power law elasticities better reproduce the complementary relationship than the arc elasticities.

436 We observed that the statistical models considered by Xiao et al. (2020) failed to produce
437 reasonable values of ε_{PET} for multiple basins. The statistical estimates of elasticities of Xiao et al.
438 (2020) are all based on arc elasticity and are termed Xiao-OLS and Xiao-GLS Besides the two
439 statistical models, they also considered a physical model referred to as Xiao-USGS which is neither
440 an arc elasticity nor a power law elasticity. Rather, it should be thought of as the best possible
441 estimate of true elasticity in equation (1). It should be noted that Xiao-OLS model is same as the
442 at-site OLS model considered in this study. Based on their study, Xiao et al. (2020) expressed a
443 need of a robust estimator of PET elasticity (i.e., ε_{PET}). We also noted that the statistical models
444 of Xiao et al. (2020) could not produce the DCR for basins with high coefficient of variation in
445 streamflow (Figure S2).

446 In Figure 3 we compare power law elasticities based on OLS, Panel and Hierarchical with
447 aridity index, with the arc elasticities estimated using Xiao-OLS, Xiao-GLS and finally to the best
448 estimate based on Xiao-USGS water balance model. Figures 3a and 3b compare the cumulative
449 density functions (CDFs) plots of P and PET elasticities for the selected six models. Log-OLS and
450 Log-Panel models produce a similar precipitation elasticity estimate as Xiao-OLS and Xiao-GLS.
451 Their variation in elasticity is larger than the remaining three models. Xiao et al. (2020) mentioned
452 a limitation of their statistical models in estimating potential evapotranspiration elasticity (ε_{PET})
453 because Xiao-OLS and Xiao-GLS models produced positive values for ε_{PET} for almost half of the
454 stations which are unrealistic values. We now realize from this study that the reason for the poor
455 performance of Xiao-OLS and Xiao-GLS was because they employed the arc elasticity definition
456 instead of the power law definition. The ε_{PET} estimates from log-hierarchical model with aridity

index as a predictor are in the expected range (Figure 3b), and its CDF appear being closer to the Xiao-USGS model estimates. Importantly Figure 3c illustrates that the three power law elasticity estimators proposed in this study yield a sum of precipitation and PET elasticity estimates very close to 1 (Figure 3c). Furthermore, our statistical estimates of power law elasticity preserved Dooge's complementary relationship even better than the Xiao-USGS model (Figure 3d).

Based on the ability to preserve the DCR, we infer that power law Hierarchical model with log-aridity index as predictor has the least $AARE$ among all estimators. Thus, we consider that model alone for understanding the relationship between the physical attributes of the basin and climate elasticities. In Figure 4, we show a correlation matrix plot between climate elasticity estimates from the selected power law Hierarchical approach and four basin attributes with aridity index (AI) and basin drainage area (DA) in log-transformed scale due to their high skewness. The two P and PET climate elasticities share a perfect negative correlation as expected. The correlation of elasticities is also significant with three basin attributes namely AI, DA and CR. Precipitation/potential evapotranspiration elasticity exhibit a perfect positive/negative correlation with AI because of the model formulation. This suggests that runoff is more sensitive to precipitation and potential evapotranspiration in arid basins and a unit change in them will change runoff by a larger factor than in humid basins. A significant negative correlation between AI and CR suggests that arid basins in the Western U.S. region experience moisture and energy being in out of phase. A similar correlation matrix plot is also developed for the power law Panel model (Figure S3) where both the considered climate elasticities are found to be statistically significant with AI and CR as well.

Figure 5 illustrates estimated power law climate elasticities from the Log-Hierarchical (AI) Model on a U.S. map. Runoff is observed to be more sensitive to precipitation in arid basins which

480 are in the southern part of the region. These results also match the findings of Xiao et al., 2020,
481 who found arid basins are found to be more sensitive than humid basins to potential
482 evapotranspiration. Figure 5c shows the deviation from Dooge's complementary relationship
483 which illustrates that humid basin in the north over-estimate, whereas arid basins in the south
484 underestimate the complementary relationship.

485 # 5.0 Discussion

486 Given the challenges in estimating the sensitivity of streamflow using climate change
487 projections, we developed an advanced, alternate observational evidence-based approach to
488 estimation of climate elasticity of streamflow. We propose two new regional climate elasticity
489 models, a panel model and a hierarchical model, to estimate both regional (ε_P^R, ε_{PET}^R) and basin-
490 specific ($\varepsilon_P^R + \varepsilon_{P,}^b$ $\varepsilon_{PET}^R + \varepsilon_{PET}^b$) P and PET elasticities and compare their ability to preserve DCR.
491 In general, none of the arc elasticity estimators were able to reproduce the DCR, hence such
492 approaches should no longer be considered for climate elasticity estimation. This is a new result
493 and given the dearth of applications of arc climate elasticity in previous studies, it is important to
494 consider the implications of our findings. For example, all the statistical methods employed by
495 Xiao et al. (2019) employed arc elasticity as opposed to power law elasticities which is the primary
496 reason none of the statistical models proposed in Xiao et al., (2020) could reproduce the DCR.

497 Our analyses show that the power law elasticities estimated using a hierarchical model
498 performed best in preserving the DCR, yet both the panel model and at-site OLS models also
499 performed equally well in estimating DCR. Basin characteristics (Figure 4), moisture-energy phase
500 relationship (CR) and elevation (EL), show statistically significant relationship between P and PET
501 elasticities, but aridity index is the primary basin characteristic accounting for the spatial variation

in the climate elasticity. Based on Figure 5, ε_P and $|\varepsilon_{PET}|$ of basins in arid basins in Region 18 are higher than those in humid/semi-humid basins in Region 17. By developing a regional model that has both a regional estimate ($\varepsilon_\cdot^R$) and also accounts for the local basin response to climate ($\varepsilon_\cdot^b$) based on AI resulted in preserving the DCR based on the power law elasticity. Similarly, the panel model performs equally well and also provides a regional value of elasticities. The regional values (ε_P^R) of the precipitation elasticity for the hierarchical model and panel model are 1.388 and 1.270 respectively, whereas the regional values (ε_{PET}^R) of potential evapotranspiration elasticity for the hierarchical model and panel models are -0.46 and -0.33 respectively. Even though at-site OLS of the power law elasticity performs well in comparison to the regional panel and hierarchical power law elasticities, a critical advantage of the regional models is that they provide a regional sensitivity of streamflow to climate, which could help in understanding the large-scale vulnerability of water availability of climate change. Further, these regional models also eliminate the need to convert the point estimates to regional estimates or elasticity contours at a regional/continental scale (e.g., Figure 4 in Sankarasubramanian et al., 2001). Thus, we recommend utilizing either a panel or hierarchical power law elasticity approach for analyzing the sensitivity of streamflow at a regional/continental scale.

To understand how regional elasticities change over different regions, we recalibrated both panel-and -hierarchical models again to estimate the power law elasticity for the Pacific Northwest (Region 17) and California HUC2 (Region 18) regions which resulted in a total of 82 watersheds (i.e., leaving out two basins in the Great Basin Region). Based on this, the estimated regional *P* elasticities ε_P^R were 1.14 and 1.19 (1.57 and 1.38) for the panel and hierarchical models respectively for the Pacific Northwest (California) region. Thus, in the humid/semi-humid northwest, *P* elasticities are closer to each other because the aridity index of the basins does not

vary much. In contrast, in the arid/semi-arid California region, the panel model indicates higher P elasticity estimates compared to the hierarchical model. Similarly, the estimated ε_{PET}^{R} were -0.20 and -0.29 (-0.63 and -0.45) for the panel and hierarchical model for the Pacific Northwest (California) region. The regional potential evapotranspiration elasticity is closer for the Pacific Northwest as opposed to the California region. These findings are consistent with the Budyko-curve estimates of precipitation elasticity, which do not vary much for humid basins, but vary significantly for arid basins (See Figure 8 in Sankarasubramanian et al., 2001).

6.0 Concluding Remarks

Investigating the sensitivity of streamflow to climate using observational data has become crucial due to underlying uncertainties in climate change projections and subsequent model-chains, an approach which introduces considerable additional errors and uncertainties (see Seo et al., 2016). Given this, many studies have proposed different empirical estimators of climate elasticity of streamflow under two different definitions of elasticity– power law elasticity (or log-linear model) and arc elasticities – and importantly, nearly all previous elasticity studies have not evaluated the ability of estimated climate elasticities to preserve Dooge's complementary relationship (DCR) ($\varepsilon_P + \varepsilon_{PET} = 1$). Motivated by the study by Xiao et al., (2020), we compared these two definitions of climate elasticity, i.e., arc elasticity and power-law elasticity, by developing statistical models using three different estimators namely at-site OLS, Regional Panel, and Regional Hierarchical models. We used four basin attributes to develop four individual hierarchical models (i.e., AI, DA, EL, and CR), thus obtained ε_P and ε_{PET} from twelve models for 84 basins considered in Xiao et al. (2020).

We found that all models provide comparable estimates of ε_P but those corresponding estimates of ε_P differed substantially between arid and humid basins. Further, using arc-elasticities positive values for ε_{PET} (which are physically unrealistic) resulted at more than half of the basins which was not the case with the power-law elasticities. Our findings suggest that estimators of power law elasticities not only preserve the DCR better than arc elasticities, but also provide reasonable estimates of ε_{PET}. Hence, we suggest future studies should only consider power law models as opposed to the conventional arc elasticities because the former provides more reasonable estimates for ε_{PET} and also preserves DCR. Regional panel-and-hierarchical estimators proved to be quite robust modeling techniques for estimating regional as well as basin scale climate elasticities. The Hierarchical power law elasticities with aridity index is found to be the best performing approach for preserving the DCR in comparison to the DCR estimates obtained from the Panel power law elasticities and even the USGS water balance model considered by Xiao et al., (2020). Our analysis also indicates that regional climate elasticity of the basins located in arid/semi-arid California region (in comparison to Pacific Northwest) are more sensitive to climate, which also agrees with theoretical elasticity curves based on the Budyko curves. Though we limited our current work to the western U.S. region, the regional panel and hierarchical models proposed in this study should be applied across different regions of the U.S. and elsewhere. Such analyses will not only help in understanding the climate elasticity of streamflow over each region but will also eliminate the need to convert the basin estimates to regional estimates because both, panel and hierarchical estimators of power law elasticity, directly provide regional elasticity estimates. The proposed regional elasticity formulation also provides basin-specific estimates which provides an opportunity to relate the within-region differences to basin attributes.

Open Research

The data used in this study is obtained from Xiao et al. (2020) and which is also archived at https://doi.org/10.6084/m9.figshare.10278089.

Acknowledgements

Chandramauli Awasthi was supported by NSF grants # CBET-1805293 and 2208562.

References

1. Allaire, M. C., Vogel, R. M., & Kroll, C. N. (2015). The hydromorphology of an urbanizing watershed using multivariate elasticity. Advances in water resources, 86, 147-154.
2. Andréassian, V., Coron, L., Lerat, J., & Le Moine, N. (2016). Climate elasticity of streamflow revisited–an elasticity index based on long-term hydrometeorological records. Hydrology and Earth System Sciences, 20(11), 4503-4524.
3. Andreyeva, T., Long, M. W., & Brownell, K. D. (2010). The impact of food prices on consumption: a systematic review of research on the price elasticity of demand for food. American journal of public health, 100(2), 216-222.
4. Bassiouni, M., Vogel, R. M., & Archfield, S. A. (2016). Panel regressions to estimate low-flow response to rainfall variability in ungaged basins. Water Resources Research, 52(12), 9470-9494.
5. Berghuijs, W. R., Larsen, J. R., Van Emmerik, T. H., & Woods, R. A. (2017). A global assessment of runoff sensitivity to changes in precipitation, potential evaporation, and other factors. Water Resources Research, 53(10), 8475-8486.
6. Blum, A. G., Ferraro, P. J., Archfield, S. A., & Ryberg, K. R. (2020). Causal effect of impervious cover on annual flood magnitude for the United States. Geophysical Research Letters, 47(5), no-no.
7. Brown, C., Meeks, R., Hunu, K., & Yu, W. (2011). Hydroclimate risk to economic growth in sub-Saharan Africa. Climatic Change, 106(4), 621-647.
8. Chiew, F. H. (2006). Estimation of rainfall elasticity of streamflow in Australia. Hydrological Sciences Journal, 51(4), 613-625.
9. De Leeuw, J., Meijer, E., & Goldstein, H. (2008). Handbook of multilevel analysis. New York: Springer.
10. Dooge, J. C. (1992). Sensitivity of runoff to climate change: A Hortonian approach. Bulletin of the American Meteorological Society, 73(12), 2013-2024.

11. Dooge, J. C. I., Bruen, M., & Parmentier, B. (1999). A simple model for estimating the sensitivity of runoff to long-term changes in precipitation without a change in vegetation. Advances in water resources, 23(2), 153-163.
12. Fang, S., Johnson, J. M., Yeghiazarian, L., & Sankarasubramanian, A. (2023). Improved National-Scale Flood Prediction for Gauged and Ungauged Basins using a Spatio-temporal Hierarchical Model. Authorea Preprints.
13. Fernandez, W., Vogel, R. M., & Sankarasubramanian, A. (2000). Regional calibration of a watershed model. Hydrological sciences journal, 45(5), 689-707.
14. Ferreira, S., & Ghimire, R. (2012). Forest cover, socioeconomics, and reported flood frequency in developing countries. Water resources research, 48(8).
15. Goldstein, H. (2011). Multilevel statistical models (Vol. 922). John Wiley & Sons.
16. Hargreaves, G. H. (1975). Moisture availability and crop production. Transactions of the ASAE, 18(5), 980-0984.
17. Hirsch, R. M., & De Cicco, L. A. (2015). *User guide to Exploration and Graphics for RivEr Trends (EGRET) and dataRetrieval: R packages for hydrologic data* (No. 4-A10). US Geological Survey.
18. Izady, A., K. Davary, A. Alizadeh, B. Ghahraman, M. Sadeghi and A. Moghaddamnia, (2012). Application of "panel-data" modeling to predict groundwater levels in the Neishaboor Plain, Iran, Hydrogeology Journal, 20(3):435-447, DOI: 10.1007/s10040-011-0814-2
19. Johnson, J. M., Fang, S., Sankarasubramanian, A., Rad, A. M., da Cunha, L. K., Clarke, K. C., ... & Yeghiazarian, L. (2023). Comprehensive analysis of the NOAA National Water Model: A call for heterogeneous formulations and diagnostic model selection.
20. Kirschen, D. S., Strbac, G., Cumperayot, P., & de Paiva Mendes, D. (2000). Factoring the elasticity of demand in electricity prices. IEEE Transactions on Power Systems, 15(2), 612-617.
21. Konapala, G., and A.K. Mishra, (2016). Three-parameter-based streamflow elasticity model: Application to MOPEX basins in the USA at annual and seasonal scales. Hydrology and Earth System Sciences, 20(6), 2545–2556. https://doi.org/10.5194/hess-20-2545-2016
22. Lerner, A. P. (1933). The diagrammatical representation of elasticity of demand. The Review of Economic Studies, 1(1), 39-44.
23. Levy, M. C., A.V. Lopes, A. Cohn, L.G. Larsen, and S.E. Thompson, (2018). Land use change increases streamflow across the arc of deforestation in Brazil. Geophysical Research Letters, 45, 3520–3530. https://doi.org/10.1002/2017GL076526
24. Milly, P. C., & Dunne, K. A. (2011). On the hydrologic adjustment of climate-model projections: The potential pitfall of potential evapotranspiration. Earth Interactions, 15(1), 1-14.
25. Over, T.M., Saito, R.J., and Soong, D.T., (2016). Adjusting annual maximum peak discharges at selected stations in northeastern Illinois for changes in land-use conditions: U.S. Geological Survey Scientific Investigations Report 2016–5049, 33 p., http://dx.doi.org/10.3133/sir20165049.
26. Padrón, R. S., Gudmundsson, L., Greve, P., & Seneviratne, S. I. (2017). Large-scale controls of the surface water balance over land: Insights from a systematic review and meta-analysis. Water Resources Research, 53(11), 9659-9678.

27. Penman, H. L. (1948). Natural evaporation from open water, bare soil and grass. Proceedings of the Royal Society of London. Series A. Mathematical and Physical Sciences, 193(1032), 120-145.
28. Pinheiro, J., Bates, D., DebRoy, S., Sarkar, D., & R Core Team. (2021). nlme: Linear and Nonlinear Mixed Effects Models. https://CRAN.R-project.org/package=nlme
29. Sankarasubramanian, A., D. Wang, S. Archfield, M. Reitz, R.M. Vogel, A. Mazrooei, and S. Mukhopadhyaya, (2020). HESS opinions: Beyond the long-term water balance: Evolving Budyko's legacy for the Anthropocene towards a global synthesis of land-surface fluxes under natural and human-altered watersheds. Hydrology and Earth System Sciences Discussions, 24(4). https://doi.org/10.5194/hess-2019-418
30. Sankarasubramanian, A., Vogel, R. M., & Limbrunner, J. F. (2001). Climate elasticity of streamflow in the United States. Water Resources Research, 37(6), 1771-1781.
31. Schaake, J.C., (1990). From climate to flow. In: Waggoner, P.E. (ed.), Climate Change and U.S. Water Resources, John Wiley, New York, pp. 177–206 (Chapter 8).
32. Seo, S. B., Sinha, T., Mahinthakumar, G., Sankarasubramanian, A., & Kumar, M. (2016). Identification of dominant source of errors in developing streamflow and groundwater projections under near-term climate change. Journal of Geophysical Research: Atmospheres, 121(13), 7652-7672.
33. Singh, D., Jain, S. K., & Gupta, R. D. (2015). Statistical downscaling and projection of future temperature and precipitation change in middle catchment of Sutlej River Basin, India. Journal of Earth System Science, 124, 843-860.
34. Steinschneider, S., Y.-C.E. Yang, and C. Brown, (2013). Panel regression techniques for identifying impacts of anthropogenic landscape change on hydrologic response. Water Resources Research, 49, 7874–7886. https://doi.org/10.1002/2013WR013818.
35. Vogel, R. M., Wilson, I., & Daly, C. (1999). Regional regression models of annual streamflow for the United States. Journal of Irrigation and Drainage Engineering, 125(3), 148-157.
36. Vogel, R. M., Tsai, Y., & Limbrunner, J. F. (1998). The regional persistence and variability of annual streamflow in the United States. Water Resources Research, 34(12), 3445-3459.
37. Wang, W., S. Zou, Q. Shao, W. Xing, X. Chen, X. Jiao, Y. Luo, B. Yong, and Z. Yu, (2016). The analytical derivation of multiple elasticities of runoff to climate change and catchment characteristics alteration. Journal of Hydrology, 541, 1042–1056. https://doi.org/10.1016/j.jhydrol.2016.08.014
38. Wood, A. W., & Lettenmaier, D. P. (2006). A test bed for new seasonal hydrologic forecasting approaches in the western United States. Bulletin of the American Meteorological Society, 87(12), 1699-1712.
39. Worthington, A.C., H. Higgs, and M. Hoffmann, (2009). Residential water demand modeling in Queensland, Australia: a comparative panel data approach, Water Policy, 11(4): 427-441.
40. Xiao, M., M. Gao, R.M. Vogel, and D.P. Lettenmaier, (2020). Runoff and evapotranspiration elasticities in the Western United States: Are they consistent with Dooge's complementary relationship?. Water Resources Research, 56, e2019WR026719. https:// doi.org/10.1029/2019WR026719
41. Xu, X., D. Yang, H. Yang, and H. Lei, (2014). Attribution analysis based on the Budyko hypothesis for detecting the dominant cause of runoff decline in Haihe basin, Journal of Hydrology,m 510, 530-540.

42. Yaffee, R. (2003). A primer for panel data analysis. Connect: Information Technology at NYU, 8(3), 1-11.
43. Zhang, X., Tang, Q., Zhang, X., & Lettenmaier, D. P. (2014). Runoff sensitivity to global mean temperature change in the CMIP5 models. Geophysical Research Letters, 41, 5492–5498. https://doi.org/10.1002/2014GL060382
44. Zhou, S., Yu, B., Huang, Y., & Wang, G. (2015). The complementary relationship and generation of the Budyko functions. Geophysical Research Letters, 42(6), 1781-1790.

738 *Table 1: Performance comparison AARE defined as average absolute relative error associated*
739 *with reproduction of Dooge's complementary relation (equation 10) ($\varepsilon_{Pi} + \varepsilon_{PETi} - 1$) across 84*
740 *basins for various statistical estimators for predicting climate elasticity based on arc elasticity*
741 *and power-law elasticities, and corresponding values of R^2 for each approach*

Statistical model / Elasticity Estimation Model Form	**AARE**		**R^2**	
	Arc Elasticity	**Power Law Elasticity**	**Arc Elasticity**	**Power Law Elasticity**
At-site (OLS)	0.561	0.063	0.780	0.954
Panel Model	0.499	0.063	0.780	0.954
Hierarchical Model (X: log-Aridity Index or AI)	0.521	0.058	0.733	0.827
Hierarchical Model (X: log-Drainage Area or DA)	0.609	0.459	0.693	0.826
Hierarchical Model (X: Elevation or El)	0.635	0.136	0.696	0.820
Hierarchical Model (X: Moisture-Energy Phase relation or CR)	0.624	0.330	0.701	0.828
Xiao et al. (2020) USGS	0.084		N/A	

742

743

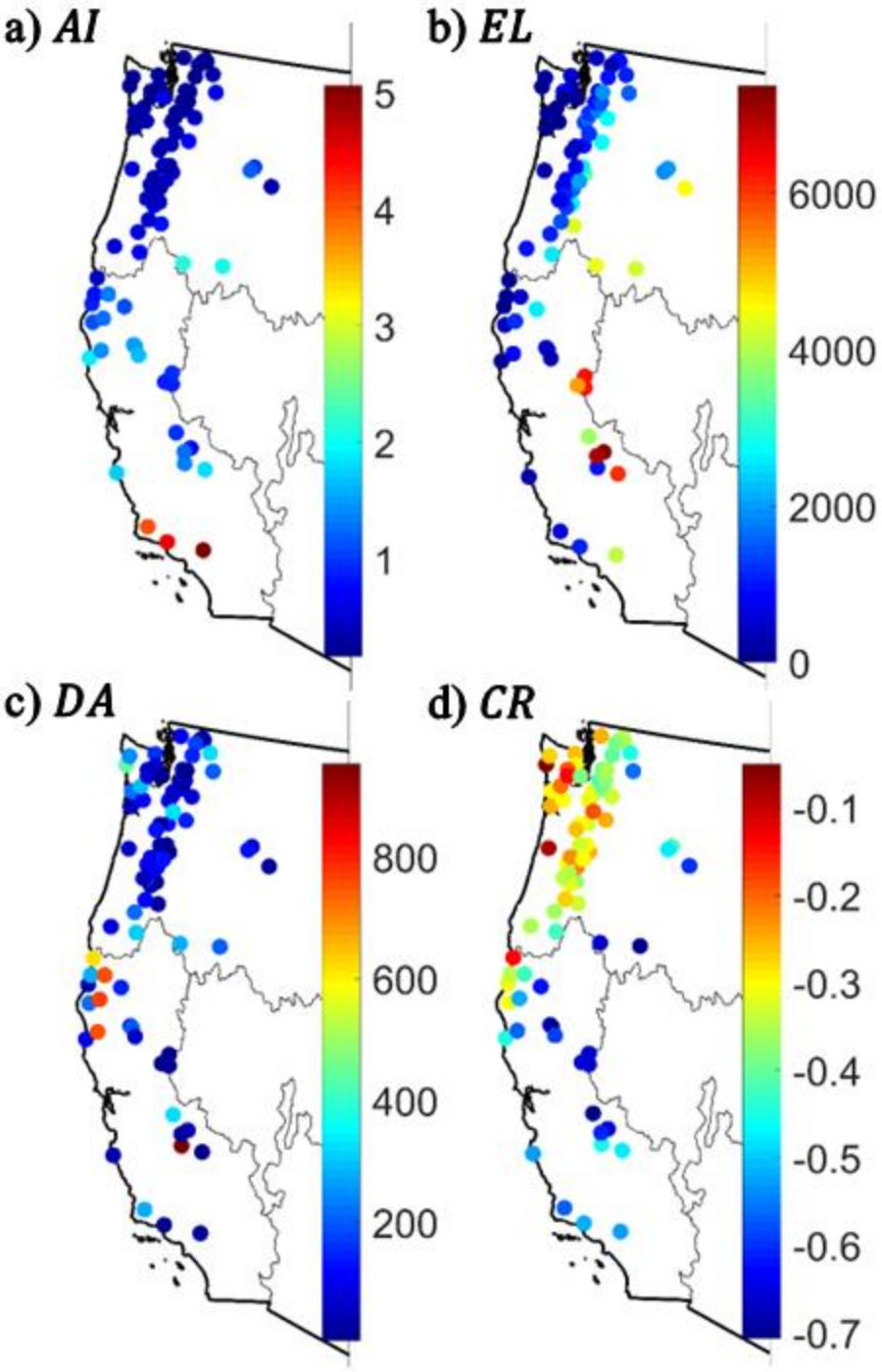

744

745 *Figure 1: Hydroclimatic and basin attributes of selected 84 basins: (a) aridity index (AI), (b)*
746 *basin gage elevation in feet (EL), (c) and basin drainage area in square-mile (DA), (d) linear*
747 *correlation coefficient between precipitation and potential evapotranspiration (CR),*

748

749

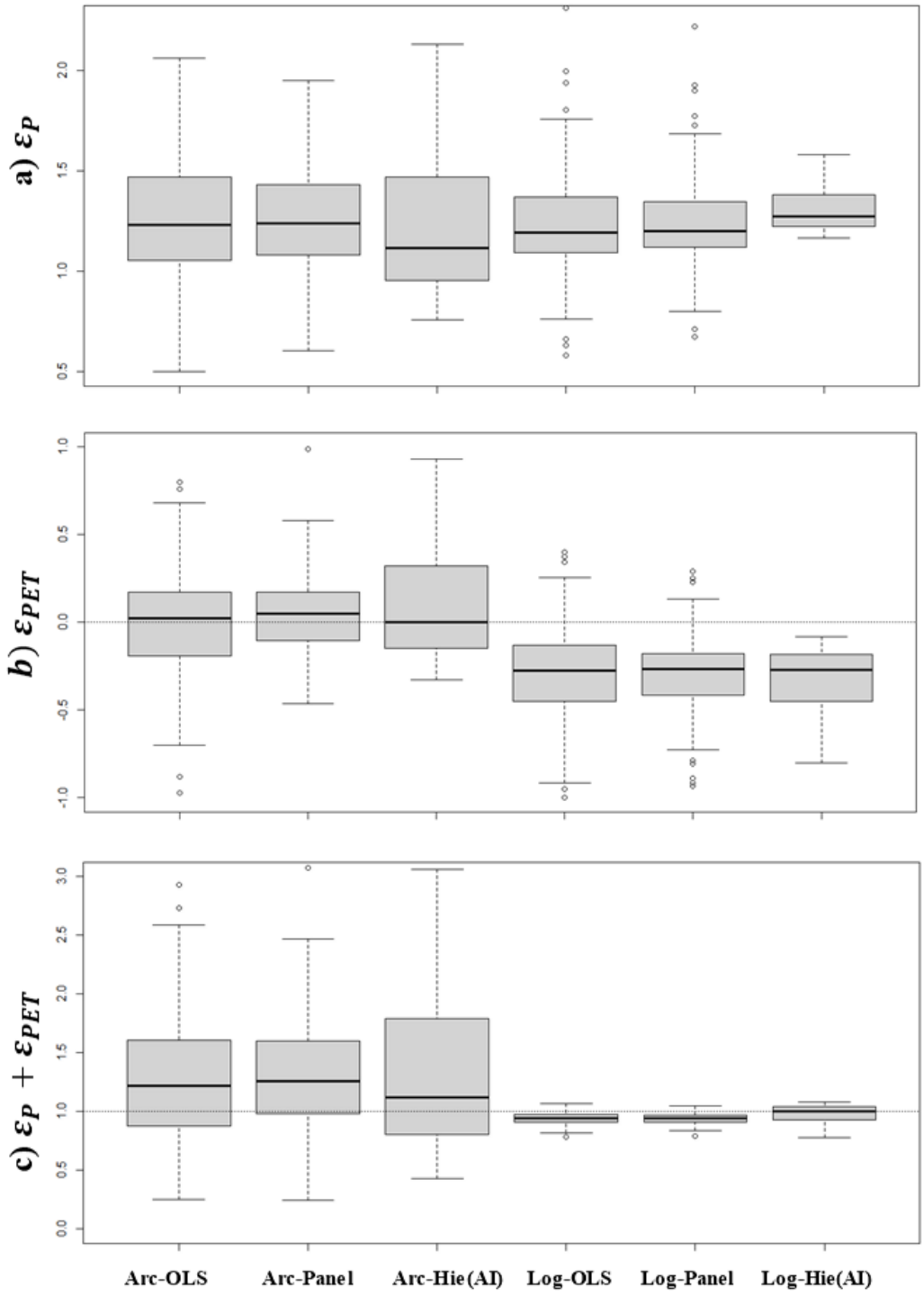

Figure 2: Boxplot of regional variation in the estimates of (a) precipitation elasticity (ε_P), (b) potential evapotranspiration elasticity (ε_{PET}), and (c) summation of those two elasticities ($\varepsilon_{PET} + \varepsilon_{PET}$, should be 1 for Dooge's complementary relation) across 84 basins from various approaches.

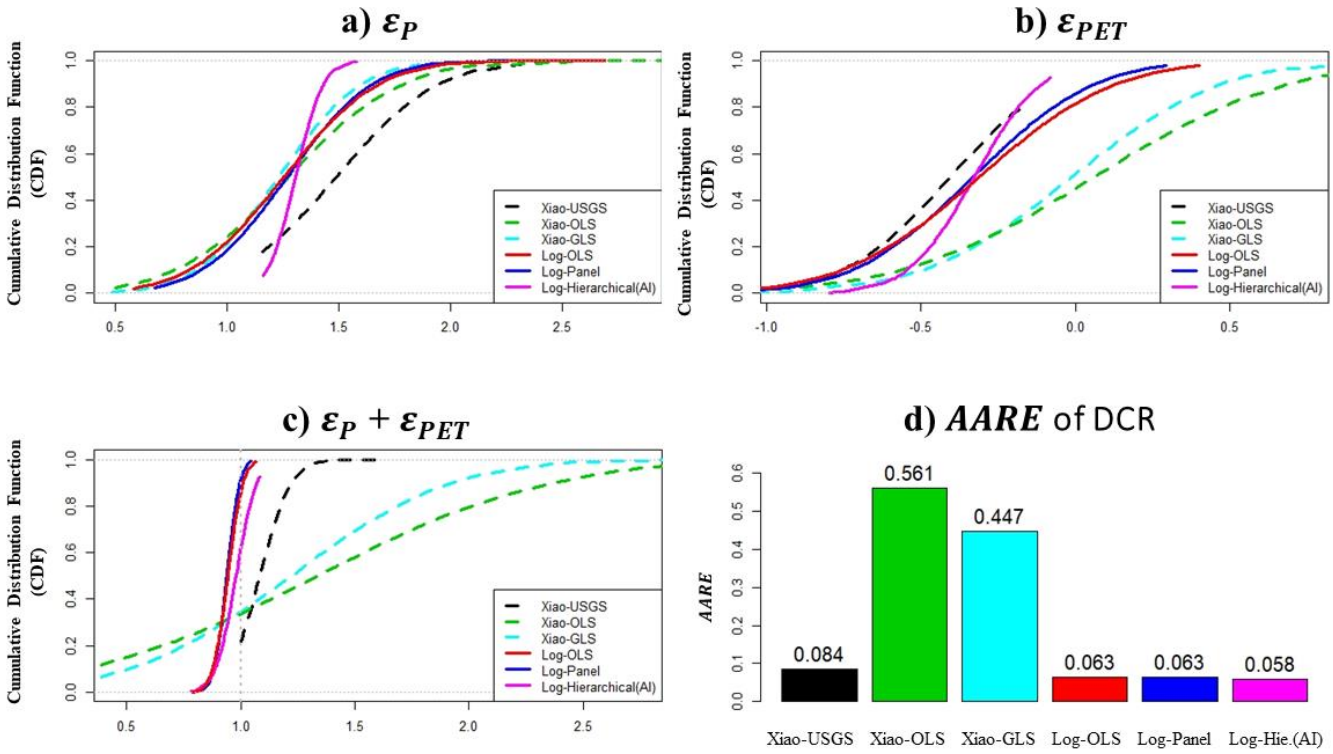

Figure 3: Comparison of power law elasticities based on Log-OLS, Log-Panel and Log-Hierarchical with aridity index, with the arc elasticities estimated using Xiao-OLS, Xiao-GLS and finally to the best estimate based on Xiao-USGS water balance model. This in estimating climate elasticities of 84 watersheds: a) CDFs of ε_P, b) CDFs of ε_{PET}, c) CDFs of $\varepsilon_P + \varepsilon_{PET}$ (should be 1 for Dooge's complementary relation to hold true), d) AARE of Dooge's complementary relation (refer Table 1 and equation 10)

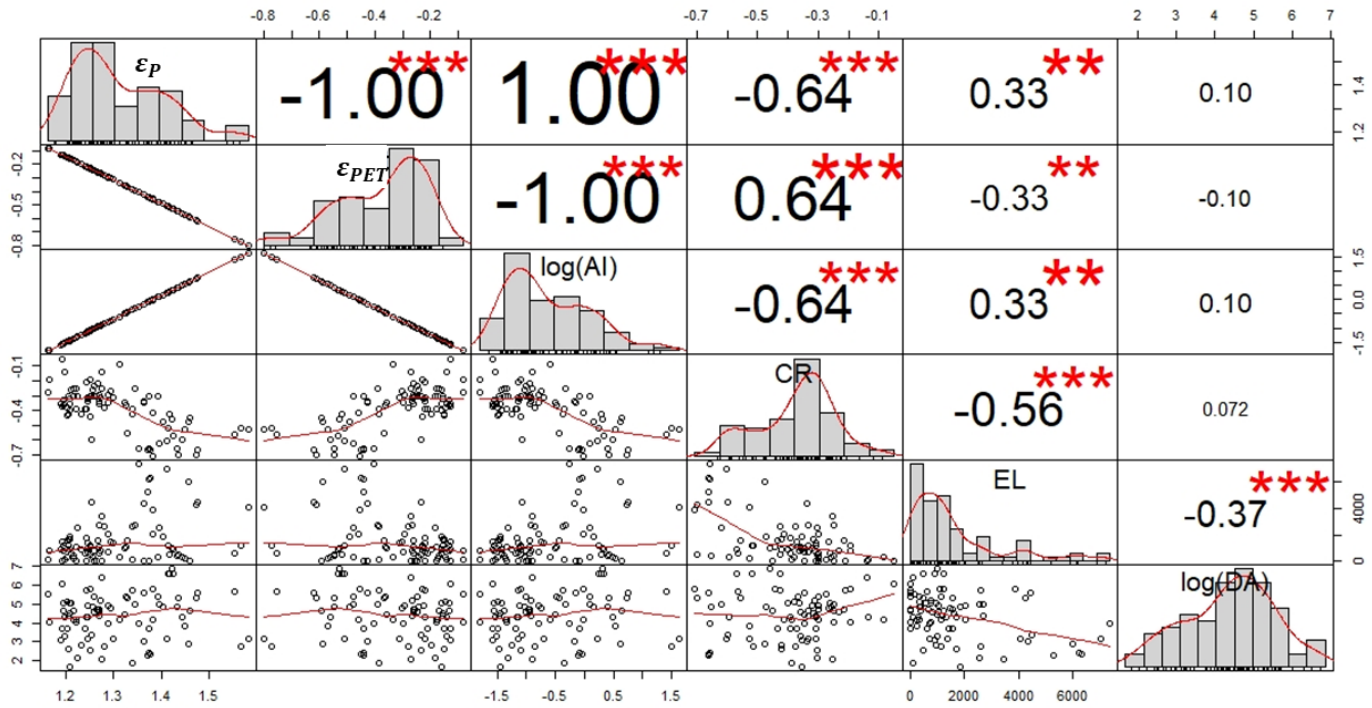

*Figure 4: Correlation matrix between climate elasticities and watershed attributes from the log-hierarchical (AI) model. ** (***) indicates the correlation at 1% (0.1%) significance level.*

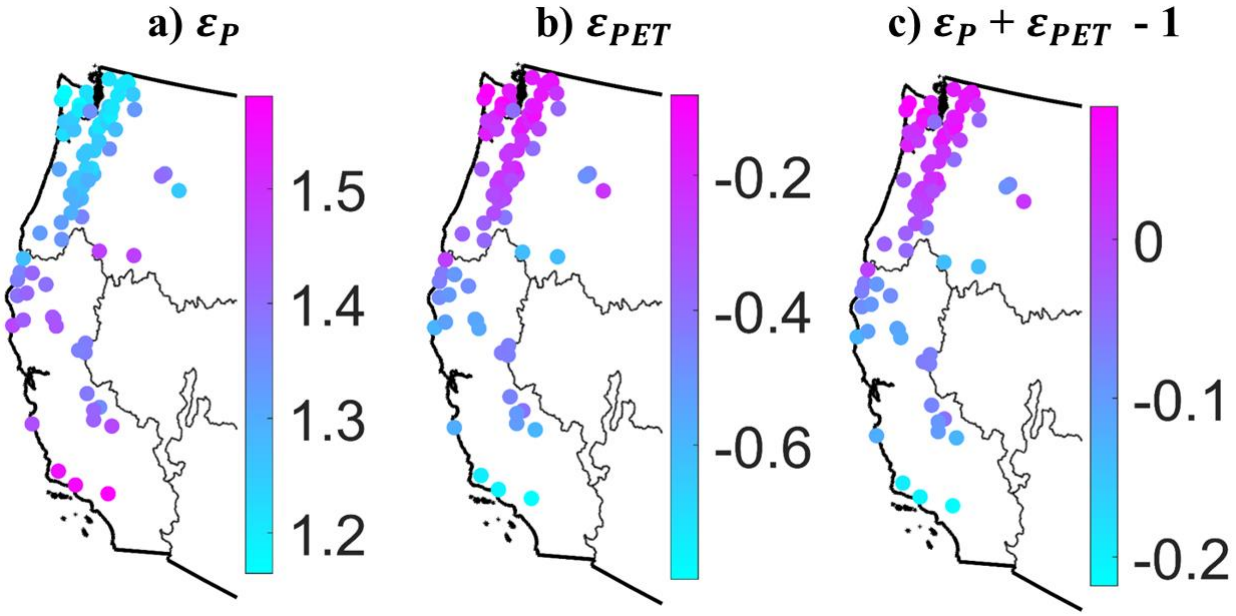

Figure 5: Spatial distribution of climate elasticities and their deviation from Dooge's complementary relation from log-hierarchical (AI) model: (a) Precipitation elasticity (ε_P), (b) Evapotranspiration elasticity (ε_{PET}), (c) Deviation from the Dooge's complementary relationship ($\varepsilon_P + \varepsilon_{PET}$ - *1*)